



# PLGA nanoparticles prepared by nano-emulsion templating using low-energy methods as efficient nanocarriers for drug delivery across the blood–brain barrier



C. Fornaguera<sup>a,b,\*</sup>, A. Dols-Perez<sup>a,b</sup>, G. Calderó<sup>a,b</sup>, M.J. García-Celma<sup>b,c</sup>, J. Camarasa<sup>d</sup>, C. Solans<sup>a,b</sup>

<sup>a</sup> Institute of Advanced Chemistry of Catalonia (IQAC-CSIC), C/Jordi Girona, 18–26 Barcelona, Spain

<sup>b</sup> CIBER of Bioengineering, Biomaterials and Nanomedicine (CIBER-BBN), Barcelona, Spain

<sup>c</sup> Department of Pharmacy and Pharmaceutical Technology, University of Barcelona, Av/ Joan XXIII s/n, 08028 Barcelona, Spain

<sup>d</sup> Department of Pharmacology and Therapeutic Chemistry (Pharmacology Section), University of Barcelona, Av/ Joan XXIII s/n, 08028 Barcelona, Spain

## ARTICLE INFO

### Article history:

Received 28 March 2015

Received in revised form 29 May 2015

Accepted 1 June 2015

Available online 6 June 2015

### Keywords:

Nano-emulsions

Polymeric nanoparticles

Loperamide

Blood–brain barrier

Active targeting

## ABSTRACT

Neurodegenerative diseases have an increased prevalence and incidence nowadays, mainly due to aging of the population. In addition, current treatments lack efficacy, mostly due to the presence of the blood–brain barrier (BBB) that limits the penetration of the drugs to the central nervous system. Therefore, novel drug delivery systems are required. Polymeric nanoparticles have been reported to be appropriate for this purpose. Specifically, the use of poly-(lactic-co-glycolic acid) (PLGA) seems to be advantageous due to its biocompatibility and biodegradability that ensure safe therapies. In this work, a novel approximation to develop loperamide-loaded nanoparticles is presented: their preparation by nano-emulsion templating using a low-energy method (the phase inversion composition, PIC, method). This nano-emulsification approach is a simple and very versatile technology, which allows a precise size control and it can be performed at mild process conditions. Drug-loaded PLGA nanoparticles were obtained using safe components by solvent evaporation of template nano-emulsions. Characterization of PLGA nanoparticles was performed, together with the study of the BBB crossing. The *in vivo* results of measuring the analgesic effect using the hot-plate test evidenced that the designed PLGA loperamide-loaded nanoparticles are able to efficiently cross the BBB, with high crossing efficiencies when their surface is functionalized with an active targeting moiety (a monoclonal antibody against the transferrin receptor). These results, together with the nanoparticle characterization performed here are expected to provide sufficient evidences to end up to clinical trials in the near future.

© 2015 Elsevier B.V. All rights reserved.

## 1. Introduction

Neurodegenerative diseases have an increased prevalence and incidence nowadays, mainly due to an aging of the population [1–4]. Current treatments lack efficacy, mostly due to the presence of the blood–brain barrier (BBB) that limits the penetration of drugs to the central nervous system [1–7]. To overcome this barrier, a promising strategy is the design of advanced BBB-targeted nanocarriers. A rational design of the nanocarriers should ensure biocompatibility, a long circulation time in the bloodstream and targeting the brain capillary endothelial cells (BCEC) producing a local pharmacological action and decreasing side effects (a characteristic drawback of current therapies). In the last decade, polymeric nanoparticles have focused an increasing interest for low-invasive treatments of neural diseases. It has been shown that the polymer characteristics as well as nanoparticle size

and surface modifications, among other factors, affect their mode of internalization by BCEC and thereby their subcellular fate and potential of crossing the epithelial cells of the BBB [1,8–13]. The nanoparticle fabrication process is also an important factor as it may affect the efficiency, safety, biodistribution and final availability of the nanocarrier. In this context, the design of polymeric nanoparticles by nano-emulsion templating stands out as a safe and versatile technique for the preparation of nanocarriers.

Nano-emulsions are emulsions with droplet sizes typically in the range of 20–200 nm. Their preparation using low-energy emulsification methods, in which the size is controlled by the intrinsic physicochemical properties of the system [14–18] allows the formation of smaller and more uniform droplets than using high-energy methods, in which droplet size is controlled by the magnitude of the external energy input. Among low-energy emulsification methods, the phase inversion composition (PIC) method is highly advantageous for systems with thermolabile compounds, such as drugs, as it can be performed at room temperature. In the PIC method, emulsification is triggered by the changes in the spontaneous surfactant curvature produced during emulsification, varying the

\* Corresponding author at: C/ Jordi Girona, 18–26, 08034 Barcelona, Spain.

E-mail addresses: [cristina.fornaguera@iqac.csic.es](mailto:cristina.fornaguera@iqac.csic.es), [cfornaguera@gmail.com](mailto:cfornaguera@gmail.com) (C. Fornaguera).

composition at constant temperature [19–23]. Polymeric nanoparticles can be obtained from nano-emulsions either by in situ monomer polymerization in the dispersed phase or using a preformed polymer (dissolved in a volatile organic solvent) as the dispersed phase of the nano-emulsion followed by solvent evaporation [9,12,24–27]. The use of biocompatible preformed polymers is advantageous over in situ monomer polymerization because the presence of reactive substances such as initiators or the generation of byproducts is avoided, thus improving the biocompatibility of the system, and reducing purification steps [12,28]. Among preformed polymers, poly-(lactic-co-glycolic acid) (PLGA) is beneficial due to its biocompatibility and biodegradability that ensure safer therapies. Its use as nanocarrier for the BBB crossing and treatment of neural diseases has also been reported previously [29–32].

The aim of the present work is to demonstrate, for the first time, that the nano-emulsion templating using the PIC method is an appropriate and simple technology to formulate nanoparticles able to deliver actives specifically to the central nervous system (CNS) by crossing the BBB. To this end, a model drug, loperamide, was chosen as a model drug without analgesic effects, since it is not able to cross the BBB. The hot-plate test was selected as the methodology to measure the central analgesia produced by our novel nanoparticle formulations, loaded with loperamide, in case they were able to cross the BBB. This methodology (hot plate test + loperamide drug use) was chosen because its suitability for the purpose of studying BBB crossing has been already reported [29–32]. In fact, bibliography reporting polymeric nanoparticles loaded with loperamide to study BBB crossing is extensive [29–32]. Specifically, the group of Kreuter and coworkers reported the results of numerous studies on central analgesia produced by polymeric nanoparticles functionalized with different compounds (e.g. polysorbate 80, targeting moieties such as monoclonal antibodies). In our work, in contrast, loperamide was loaded in PLGA-solvent mixtures prior to nano-emulsion formation, and polysorbate 80 was used as the surfactant of the template nano-emulsion, avoiding time-consuming coating steps. O/W polymeric nano-emulsions were produced and after solvent evaporation, gave rise to polymeric loperamide-loaded nanoparticles. The loperamide-loaded nanoparticles were functionalized with a monoclonal antibody against the transferrin receptor and the BBB crossing was studied in vivo.

## 2. Materials and methods

### 2.1. Materials

Poly(lactic-co-glycolic acid), Resomer 752H (PLGA) (polystyrene equivalent molecular weight PSE-MW ~10,000 g/mol, determined by Gel Permeation Chromatography) was purchased from Boehringer Ingelheim. The PLGA lactic to glycolic acid ratio was 75/25 and the end groups were free-carboxylic acids. Ethyl acetate and ethanol used as the organic volatile solvents were purchased from Merck. Polysorbate 80 was kindly provided by Croda. Loperamide hydrochloride (LOP) (MW = 513.51 g/mol,  $\lambda$  ~ 220–300 nm depending on the solvent) was bought at Sigma-Aldrich [33]. The 8D3 mouse monoclonal antibody against the transferrin receptor (8D3) was purchased from Bionova (MW = 160 kDa). *N*-(3-dimethylaminopropyl)-*N*-ethylcarbodiimide hydrochloride (EDC) was purchased from Fluka and *N*-hydroxysuccinimide sodium salt (NHS) from Sigma-Aldrich. Salts for the phosphate buffered saline (PBS, 0.16 M, pH = 7.4, 300 mOsm/kg): sodium chloride (NaCl), disodium monohydrogenphosphate dihydrate ( $\text{Na}_2\text{HPO}_4 \cdot \text{H}_2\text{O}$ ) and sodium dihydrogenphosphate monohydrate ( $\text{NaH}_2\text{PO}_4 \cdot \text{H}_2\text{O}$ ) were purchased from Merck. Water was MilliQ filtered (Millipore). CD1 male mice of around 30–35 mg were bought from Harlan.

### 2.2. Methods

#### 2.2.1. Preparation of O/W polymeric nano-emulsions

Nano-emulsions were prepared by stepwise addition of PBS to mixtures of surfactant (Polysorbate 80) and oil consisting of ethanol/ethyl

acetate 20/80, containing 4 wt.% of PLGA, without or with 0.1 wt.% of LOP, at 25 °C.

The region of O/W nano-emulsion formation in the pseudoternary water/surfactant/oil phase diagram was assessed visually: samples with transparent, translucent or slight opaque aspect, having a bluish or reddish shine were considered nano-emulsions. To confirm the visual assessment of nano-emulsions, their size was also characterized by dynamic light scattering, as described below (Section 2.2.3).

#### 2.2.2. Nanoparticle preparation from nano-emulsion templating

Nanoparticle dispersions were formed from nano-emulsions by the solvent evaporation method under reduced pressure [28], using a Büchi R-215V Rotavapor. The evaporation conditions used for 4 g of nano-emulsion at 25 °C were: vacuum of 43 mbars with a rotation speed of 150 rpm for 45 min. After the evaporation step the volume was adjusted with MilliQ water to maintain the osmolality of the sample around 300 mOsm/kg.

For in vitro and in vivo studies, nanoparticles were concentrated to reach therapeutic LOP concentrations. The concentration step was performed using the Centriprep® YM-3, 3 kDa, centrifugal filter units (Millipore). After this step, a 24 h dialysis was required to return to physiological pH and osmolality values (pH = 7.4 and osmolality = 300 mOsm/kg).

The following codification was assigned to nano-emulsions and corresponding nanoparticles: dispersion type (loading, functionalization), in which NE or NP are the dispersion types; 0 and 0.1 are the percentage of loperamide loading; and 8D3 is the functionalization. As an example, NP (0.8D3) refers to non-loaded nanoparticles functionalized with 8D3 antibody.

#### 2.2.3. Physico-chemical characterization of nano-emulsions and nanoparticles

The mean droplet size and size distribution of nano-emulsions and nanoparticles were determined by dynamic light scattering (DLS) using a spectrometer (LS Instruments, 3D cross correlation multiple-scattering) equipped with a He–Ne laser (632.8 nm) at a scattering angle of 90° and 25 °C. Data were treated by cumulant analysis [34]. The results are the mean of, at least, three measurements which were performed at the Nanostructured Liquid Characterization Unit of the Spanish National Research Council (CSIC) and the Biomedical Networking Center (CIBER-BBN), located at IQAC-CSIC.

The zeta potential of the nanoparticles was assessed by Electrophoretic mobility measurements with Zetasizer NanoZS instrument (Malvern Co. Ltd., UK), equipped with a He–Ne laser ( $\lambda$  = 633 nm). The zeta potential ( $\zeta$ ) was calculated from the electrophoretic mobility applying the Hückel–Onsager equation [35] (Eq. (1)):

$$\mu = \frac{3 \cdot \zeta \cdot \epsilon_r \cdot \epsilon_0}{2 \cdot \eta} \quad (1)$$

where  $\epsilon_r$  represents the relative dielectric constant of water,  $\epsilon_0$  is the vacuum permittivity and  $\eta$  is the viscosity of the liquid. As this equation is only valid if the mobility is low, samples were diluted 1:20 with distilled water.

The stability of designed nano-emulsions and nanoparticles was assessed by visual observation of macroscopic changes with time, at 25 °C.

#### 2.2.4. Loperamide quantification assays

For the analysis of LOP, a Breeze™2 HPLC (Waters Corporation, Milford, MA, USA) equipped with a 0.5 cm × 15 cm × 0.46 cm Spherisorb1 ODS column was used, and the UV detector set at 220 nm, the maximum absorption of LOP [36]. Retention time of loperamide was ~42 min. The mobile phase used was 1.824 mM of orthophosphoric acid/acetonitrile (50/50% v/v), at a pH = 3.5 and a temperature of 30 °C. The flow rate

was set at 1 mL/min, injecting 50  $\mu$ L volume of sample, and each chromatogram was plotted for 50 min.

#### 2.2.5. Entrapment efficiency and drug loading determination

The efficiency of LOP entrapment and drug loading in the nanoparticle dispersion was determined by centrifuging drug-loaded nanoparticles using centrifugal filter units with a molecular weight cut-off of 3000 Da (Amicon Ultra-15 Centrifugal Filter Unit with Ultracell-3 Membrane, Millipore, Billerica, Massachusetts, USA) and analyzing the filtrate by HPLC as specified above to determine the free drug. The centrifugation was carried out at 2300 g during 75 min at 25 °C. The drug entrapment efficiency and the drug loading were calculated using Eqs. (2) and (3), respectively [37,38].

$$\text{Entrapment efficiency (wt./wt.\%)} = \frac{\text{initial drug amount} - \text{free drug}}{\text{initial drug amount}} \times 100 \quad (2)$$

$$\text{Drug loading (g/g)} = \frac{\text{amount of drug in nanoparticles}}{\text{g of PLGA}} \quad (3)$$

#### 2.2.6. In vitro release experiments

The dialysis bag method was used, as described elsewhere [39]. Thermo jacketed glasses were used to maintain the desired temperature (25 °C). They were filled with the receptor solution, which consisted in 50 mL of milliQ water. Spectra/Por® Float-A-Lyzer® G2 (Spectrum®Labs) devices with a membrane composed of Biotech Grade Cellulose Ester with a MWCO of 3.5–5 kDa filled with 2 mL of sample and soaked into receptor solution. Aliquots of 1 mL of the receptor solution were withdrawn at controlled intervals of time and their LOP concentration assessed by HPLC as described in Section 2.2.4.

#### 2.2.7. Nanoparticle surface functionalization

Nanoparticle surface was functionalized with 8D3 antibodies by means of covalent attachment between the carboxylic groups of the PLGA polymer and the amine groups of the antibody, using the carbodiimide reaction, as described elsewhere (e.g. Fornaguera, 2015). The 8D3 antibody is a monoclonal antibody against the transferring receptor, overexpressed in the BBB. Specifically, 8D3 is a mice specific antibody, selected for the in vivo experimentation with this animal specie. Consequently, 8D3-functionalized nanoparticles would target specifically the transferring receptors, overexpressed in the BBB.

Briefly, 4 g of nanoparticle dispersion were acidified with HCl 1 M (up to pH = 4.5–6). An excess of EDC and NHS was added to nanoparticles, and the mixture was stirred for around 2 h at 25 °C. After this time, 150  $\mu$ L of activated nanoparticle dispersion was basified with NaOH 1 M (up to pH = 8). 150  $\mu$ L of 8D3 anti-transferrin receptor monoclonal antibody (1 mg/mL, 0.5 mg/mL or 0.25 mg/mL, depending on the sample) was added to nanoparticles. Mixture was incubated, stirring, for 18 h, at 25 °C. This procedure was demonstrated not to affect the antibody structure and functionality. Nanoparticles were not affected by these slight pH changes.

The antibody covalent attachment to nanoparticle surface was assessed by size exclusion chromatography (SEC), using an Alliance 2695 HPLC Waters system equipped with a UV detector Waters 2996 DAD, using an Ultrahydrogel 500 column, 10  $\mu$ m, 7.8 mm  $\times$  300 mm, 10 K–400 K (Waters).

#### 2.2.8. In vitro cell viability analysis

Cell viability in the presence of nanoparticles was assessed with the 3-(4,5-dimethylthiazol-2-yl)-2,5-diphenyltetrazolium bromide (MTT) colorimetric assay [40,41]. For each assay, HeLa cells were seeded (about  $6 \times 10^3$  cells per well) on a 96-well plate in 200  $\mu$ L of DMEM, and cultured for 24 h at 37 °C. Then, the culture medium was replaced with samples at the required concentrations. Cells were incubated for

24 h, at 37 °C under 5% CO<sub>2</sub> atmosphere. The MTT reagent was added at a final concentration of 0.5 mg/mL (25  $\mu$ L) in PBS and incubated 2 h at 37 °C; thereafter, the medium was withdrawn and 200  $\mu$ L of DMSO was added to dissolve the formazan crystals. The plate was shaken for 15 min at room temperature. Absorbance was measured at  $\lambda$  = 570 nm with the SpectraMax M5 spectrophotometer (Molecular Devices).

#### 2.2.9. In vivo study of central analgesia

Mice were divided in groups of 4, acclimatized for 1 week and maintained with water and food ad libitum. Experimental protocols for the use of animals were approved by the Animal Ethics Committee of the University of Barcelona, following the guidelines of the European Community Council (86/609/EEC). Efforts were made to minimize suffering and reduce the number of animals used. Animals were housed at  $22 \pm 1$  °C under a 12-h light/dark cycle with free access to food (standard laboratory diet, PANLAB SL, Barcelona, Spain) and drinking water.

Adult male Swiss CD-1 mice (Charles River, Barcelona, Spain) weighing 22 to 30 g were used. Products were administered intravenously through the tail vein and injected in a volume of 5 mL/kg. Morphine was provided by the Spanish National Health Service.

Supraspinally-mediated nociception was tested using the hot-plate analgesymeter LE 7406 (PANLAB, SL, Barcelona, Spain). Mice were placed in the apparatus, which was thermostatically maintained at  $54 \pm 0.5$  °C in a precision water bath. Hot-plate latency was defined as the time interval (in seconds) between placement of the mouse onto the hot-plate and the instant a nociceptive response was elicited (e.g. licking a forepaw, jumping or hopping off the plate) [32,42,43]. Each mouse was submitted to two trials. A latency time value was recorded immediately prior to drug administration (pre-test value) and 20 min after treatment (post-test value). Mice were pre-selected, and animals with a pre-test value of more than 10 s were excluded from the study (about 10%). A cut-off time of 25 s was established [31]. Animals not responding at this time were removed from the hot-plate and given a score of 25 s.

Formulations were administered in the dose of 3 mg/kg through tail vein. The morphine and loperamide doses were equal because they have very similar affinity for the  $\mu$  opioid receptor: pK<sub>i</sub> (morphine) = 9.28; pK<sub>i</sub> (loperamide) = 9.00 [44,45]. The following formulations were used: (1) PBS solution at 0.16 M electrolyte concentration; (2) aqueous morphine at 0.7 mg/mL (3 mg morphine/kg mice); (3) NP (0); (4) NP (0.8D3); (5) NP (0.1); (6) NP (0.1, 8D3); (7) loperamide aqueous solution in 15 wt.% of polysorbate 80; and (8) aqueous solution with 15 wt.% of polysorbate 80. The concentration of loperamide in the injected solutions was 0.7 mg/mL (3 mg/kg). Results were statistically analyzed with the software SPSS Statistics 17.0. A Paired-Sample T Test was performed to compare means for each group between the pre-treatment latency times and post-treatment latency times. Moreover, the percent maximal possible effect (% MPE) was calculated with the following Eq. (4) [30–32,43]:

$$\% \text{ MPE} = \frac{\text{Post-treatment latency} - \text{Pre-treatment latency}}{\text{Cut-off time} - \text{Pretreatment latency}} \times 100\%. \quad (4)$$

### 3. Results

#### 3.1. Nano-emulsion and nanoparticle preparation and characterization

The model system PBS 0.16 M (W)/polysorbate 80 (S)/[4 wt.% PLGA in ethyl acetate] (O) was chosen as nano-emulsions with very small size (e.g. radii around 40 nm) are produced by low-energy methods [46]. Solubility studies (Table S3, SI) evidenced that a mixture of ethanol/ethyl acetate with a 20/80 weight ratio was required to incorporate 0.1 wt.% (1 mg/g oil phase) of loperamide in the nano-emulsion oil



phase (LOP solubility in the oil phase = 1.37 mg/mL = 1.56 mg/g). Therefore, polymeric nano-emulsions were prepared in the PBS 0.16 M (W)/polysorbate 80 (S)/[4 wt.% PLGA in 20/80 ethanol/ethyl acetate + x wt.% loperamide (0 or 0.1 wt.%) (O) system, using the Phase Inversion Composition (PIC) method [47]. Fig. 1 shows the region of nano-emulsion formation for non-loaded nano-emulsions and nano-emulsions containing 0.1 wt.% of loperamide. Non-loaded nano-emulsions form at O/S ratios between 35/65–95/5 and water contents above 40 wt.%, as assessed by visual observation. The addition of LOP to the system decreased slightly the nano-emulsion formation region as it comprises O/S ratios between 40/60–95/5 and water contents above 50 wt.%.

Selection of the most appropriate nano-emulsion was made after characterization of non-loaded nano-emulsions (without LOP). Nano-emulsions with 90 wt.% of aqueous phase content showed the most transparent appearance (Figure S1, SI), which is usually related with smaller droplet sizes and higher stabilities against migrational destabilization processes [16,17]. For this reason, they were chosen to determine the size and surface charge (by DLS and electrophoretic mobility, respectively) as a function of O/S ratio. The results (Fig. 2) showed that NE droplet sizes were constant, around 50 nm, as a function of the O/S ratio (Fig. 2a), up to 90/10, but at a higher O/S ratio, the size increased notably, which was attributed to insufficient surfactant concentration to stabilize the nano-emulsions (edge of the nano-emulsion formation domain). All nano-emulsions showed negative surface charges (Fig. 2b), attributed to the negative charges of the carboxylic groups of the PLGA. The lowest charges corresponded to the lower O/S ratios. Surface charge increased as a function of the O/S ratio. The inverse tendency was expected: since the origin of nano-emulsion surface charges is mainly due to the carboxylic groups of the PLGA polymer. Therefore, the higher the O/S ratio, the more negative the surface charge should be. It can be argued that a higher packing of the PLGA matrix might occur at the highest O/S ratios (higher oil percentage but same nano-emulsion size) and as a consequence the number of carboxylic groups at the nanoparticle surface might not increase.

Nano-emulsions with an O/S ratio of 70/30 were chosen as a compromise of small size (radii = 49 nm) and low surfactant content (3 wt.%). They are referred as NE (0) from now on. It is worth noting that, although the surfactant used is described to be less toxic than other types of surfactants, it is desirable to reduce the content of these components in pharmaceutical formulations to minimize possible side effects [48]. Table 1 shows the main characteristics of NE (0) and those of nano-emulsions with the same composition but including 0.1 wt.% LOP in the oil phase (referred to as NE (0.1)). The latter showed hydrodynamic radii of around 120 nm, and negative surface charges, around  $-50$  mV. The stability of both nano-emulsions (approximately 15 days) was higher than the time needed for the preparation of polymeric nanoparticles by solvent evaporation (around 1 h).

The polymeric nanoparticles NP (0) and NP (0.1), showed hydrodynamic radii around 30 nm and 100 nm respectively (Table 1) (similar to

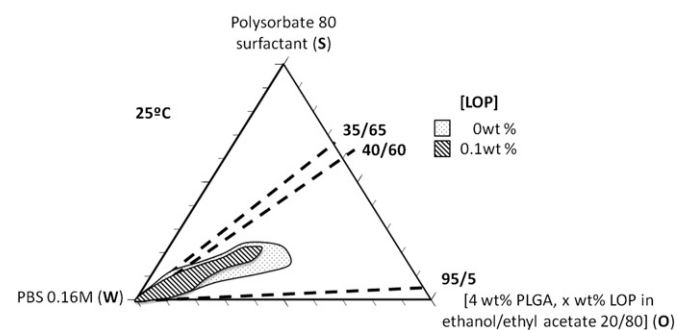


**Fig. 1.** Nano-emulsion formation region in the system: PBS 0.16 M (W)/polysorbate 80 (S)/[4 wt.% PLGA + x wt.% LOP in ethyl acetate] (O), with 0 and 0.1 wt.% of loperamide content.

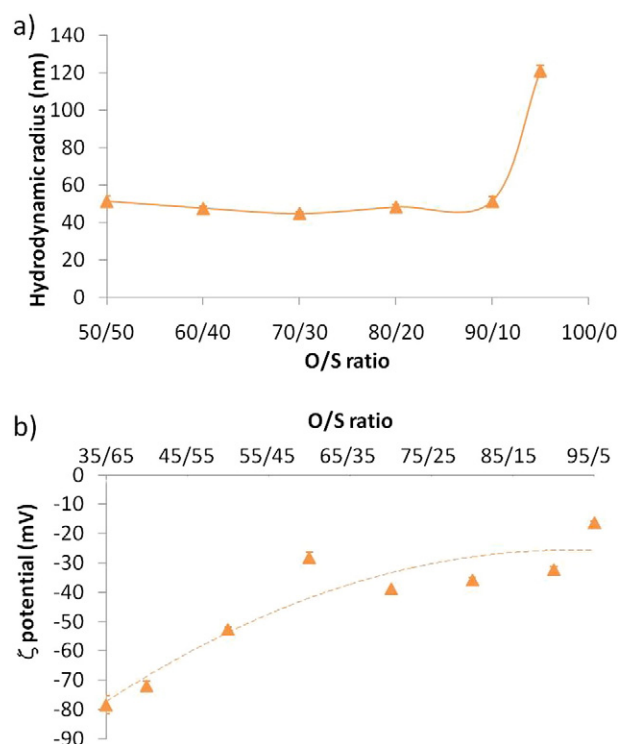


**Fig. 2.** a) Hydrodynamic droplet radii (nm) and b) zeta potential ( $\zeta$ ) (in Fig. 2b, points are the experimental results and the dash line represents a tendency) of non-loaded nano-emulsions formulated with 90 wt.% of PBS, as a function of the O/S ratio of nano-emulsions.

the sizes obtained by TEM of non-loaded PLGA nanoparticles, reported in Ref. [46]), slightly lower than those of their template nano-emulsions NE (0) and NE (0.1), attributed to evaporation of the solvent. They maintained their negative charges, due to the PLGA carboxylic groups, and showed stability higher than 3 months (Table 1).





### 3.2. Loperamide encapsulation efficiency and in vitro release

Loperamide encapsulation efficiency, assessed by the indirect filtration/centrifugation method, was higher than 99 wt.% (Table 2). This encapsulation efficiency corresponds to a loperamide loading of around 25 mg/g of PLGA and a drug concentration of 9 mg/g of nanoparticle dispersion (Table 2). This loperamide concentration is low to produce a therapeutic effect in vivo [49], unless high dispersion volumes would be administered at the as-prepared concentration, which would not be practical. Therefore, the as-prepared nanoparticles were concentrated by repeated centrifugation to achieve loperamide therapeutic doses (between 1.5–7 mg/kg) at reasonable administration volumes. A ten times concentration process was required to reach a loperamide concentration of around 0.7 mg/mL (which corresponds to 7 mg/kg when administering 300  $\mu$ L). The pH of the dispersion was not modified after nanoparticle concentration due to the buffer effect of PBS but the osmolality value increased notably. Therefore, a post-concentration dialysis was performed for 8 h (Figure S2, SI) to readjust the osmolality to physiological values (around 300 mOsm/kg). After this concentration step, zeta potential ( $\zeta$  potential) and nanoparticle sizes showed values similar to those of the as-prepared nanoparticles (Table S3, SI).

Loperamide release from the nanoparticle dispersion was compared to those from micellar and aqueous solutions. The micellar solution was a 15 wt.% Polysorbate 80 aqueous solution. This high surfactant content was needed to solubilize therapeutic concentrations of LOP, further required for in vivo experimentation. The results show (Fig. 3) that loperamide release from the aqueous solution is complete within

**Table 1**

Characteristics of loperamide-loaded nano-emulsion (NE (0.1)) and nanoparticle (NP (0.1)). The characteristics of non-loaded nano-emulsions (NE (0)) and nanoparticles (NP (0)) are also presented for comparative purposes.

Sample	Visual appearance	Visual appearance description	Hydrodynamic radius (nm)	z potential (mV)	Stability (time to sediment)
NE (0)		Transparent Bluish shine	44.73 ± 2.98	−38.70 ± 7.52	16.5 days
NE (0.1)		Translucent Slight bluish shine	119.73 ± 2.11	−51.30 ± 2.91	15 days
NP (0)		Transparent Bluish shine	30.26 ± 2.14	−36.60 ± 5.24	>90 days
NP (0.1)		Transparent Slight bluish shine	99.98 ± 2.81	−16.28 ± 0.34	>90 days

5 days, while it reaches values up to 75% from the micellar solution and around 15% from the nanoparticle dispersion within this time.

### 3.3. Antibody functionalization of nanoparticle surface

To achieve an active targeting to the blood–brain barrier (BBB), polymeric nanoparticles are functionalized with diverse components [3,30,32,50,51]. In the present work, NP (0.1) nanoparticles were functionalized with the 8D3 monoclonal antibody against the transferrin receptor, overexpressed in the BBB, using the carboxylic groups of the polymer and the amine groups of the antibody by means of the carbodiimide reaction. Three molar ratios of PLGA molecules of NP (0.1)/antibody, designated as N/P, were tested: 50/1, 25/1 and 12.5/1. As Table 3 shows, after antibody functionalization, the physico-chemical properties of nanoparticles did not vary significantly, independently of the N/P ratio, as previously reported for antibody functionalization of other types of nanoparticles [31,52].

To confirm that 8D3 antibody was attached by a covalent binding, size exclusion chromatographic (SEC) studies were performed on non-loaded nanoparticles (NP (0)). Four samples were studied: 8D3 antibody, non-loaded nanoparticles (NP (0)), non-loaded 8D3 functionalized nanoparticles (NP (0,8D3)) and a physical mixture of both components (NP (0) + 8D3). The resulting chromatograms are plotted in Fig. 4. Nanoparticles showed the maximum absorbance around 234 nm, as expected due to the presence of ester groups [66] with a retention peak at ~40 min. This peak was wide, probably due to the presence of more than one component (e.g. PLGA and surfactant) in the nanoparticle dispersion. 8D3 antibody showed the peak at a similar retention time (~42 min), but the maximum adsorption was at 279 nm, as expected for proteins [67]. For the antibody functionalized nanoparticles – NP (0,8D3), the maximum absorption was ~260 nm, showing a retention time near 55 min. The physical mixture, NP and 8D3 antibody showed the maximum absorption at 234 nm, as observed for nanoparticles, since they were the major component of the mixture. The retention time of the mixture main peak decreased to ~35 min, while a second smaller peak appeared around ~52 min. The decrease on the retention time of the physical mixture could be attributed to the spontaneous formation of bigger complexes between nanoparticles and antibodies (not covalent attachment). The presence of two peaks only in this sample (physical mixture) can be attributed to its higher polydispersity as compared with other samples, due to the coexistence between free nanoparticles, free antibodies and these hypothesized complexes. Therefore, the change in the chromatographic pattern

(absorption wavelength and retention time) enabled the confirmation of covalent antibody attachment to nanoparticle surface.

### 3.4. In vitro cytotoxicity assays

The nanoparticle cytotoxicity produced on a *HeLa* cell culture was assessed by the MTT assay. Loperamide-loaded nanoparticles (NP (0.1)), 8D3-functionalized nanoparticles (NP (0, 8D3)), and loperamide-loaded 8D3-functionalized nanoparticles, at a N/P ratio of 12.5/1 (NP (0.1, 8D3)), were studied at the as-prepared concentration (3 mg/mL), without a concentration step and also at the required therapeutic concentration (30 mg/mL), to ensure their safety in vivo. As Fig. 5 shows, cell viability was higher than 80% for all sets of nanoparticles studied, independently on the concentration, thus confirming that the formulated nanoparticles were non-cytotoxic up to a concentration of 30 mg/mL.

In vitro hemolysis tests of NP (0.1) and NP (0,8D3) nanoparticles and nanoparticle–blood protein interactions were studied previously [53]. It was shown that at a PLGA nanoparticle concentration of 30 mg/mL, both nanoparticles are non-hemolytic and interact weakly with blood components.

### 3.5. In vivo BBB crossing

To test the BBB crossing of the nanoparticles, in vivo tests on mice were performed since cell models were previously described not to accurately simulate the BBB [54]. Mice were divided in 8 groups (Table S4, SI) and treated with: NP (0.1) and NP (0.1, 8D3), as samples of interest; NP (0), NP (8D3), PBS and an aqueous micellar solution of the polysorbate 80 surfactant (referred as aqueous polysorbate 80) as negative controls since they did not contain the analgesic drug; and morphine and a micellar solution of the surfactant with 0.1 wt.% LOP (referred as

**Table 2**

Parameters related with the encapsulation of loperamide in PLGA nanoparticles.

Encapsulation efficiency (EE) (%)	99.92 ± 0.01
Drug loading (mg LOP/g PLGA)	25.23 ± 1.84
Drug concentration (mg LOP/g NPd)	9.08 ± 7 · 10 <sup>−4</sup>

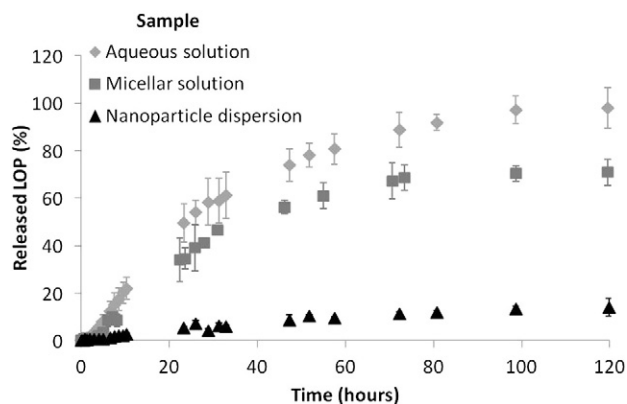


**Fig. 3.** Loperamide release (%) as a function of time, for a LOP-aqueous solution (diamonds), a LOP-micellar solution (squares) and a nanoparticle dispersion – NP (0.1) (triangles).

**Table 3**

Hydrodynamic size, zeta potential ( $\zeta$  potential) and stability (time to sediment) of 8D3-functionalized loperamide-loaded nanoparticles, NP (0.1, 8D3), as a function of NP/antibody (N/P) ratio.

N/P ratio	Hydrodynamic radius (nm)	z potential (mV)	Stability (time to sediment)
1/0	99.98 $\pm$ 2.81	−16.28 $\pm$ 0.34	>3 months
50/1	101.06 $\pm$ 3.05	−15.36 $\pm$ 4.25	>3 months
25/1	110.27 $\pm$ 5.12	−18.74 $\pm$ 0.77	>3 months
12.5/1	104.98 $\pm$ 4.32	−11.25 $\pm$ 4.56	>3 months

aqueous polysorbate 80 + LOP) as positive controls, since it is well known that morphine drug is able to cross the BBB and produce central analgesia [32], and polysorbate 80 was previously described to permeabilize the BBB, enhancing the analgesic activity at a central level [29]. Non-functionalized nanoparticles were included as a way to study the effect of the functionalization and non-loaded nanoparticles were included as a form to know the effects of the nanoparticle carrier without the active principle. It is worth noting that all mice survived after the administration of nanoparticles, for at least, one week. Although this test was not intended to determine cytotoxicity *in vivo*, the results obtained confirmed the non-toxic character of the nanoparticles, as assessed *in vitro*. The results of the nociceptive response of the treated animals are presented as the difference between the pre- and post-latency times for each set of mice studied (Fig. 6, and Table S5, SI). The time increase for the PBS sample and NP (0) was nearly null, confirming that they did not have any analgesic effect. Both positive controls (aqueous morphine and the aqueous Polysorbate 80 + LOP) resulted in significant difference between the pre- and post-latency time, with a time increase of around 10–15 s, as expected, due to the analgesia produced by morphine and LOP. Surprisingly, NP (8D3) and the aqueous micellar polysorbate 80 solution resulted in significant differences between the pre- and post-latency times, although the time increase showed lower values than those of the positive controls. Concerning the samples of interest, LOP-loaded non-functionalized nanoparticles NP (0.1) resulted in a time increase of around 7 s, clearly higher than those of negative controls, although no significant differences were found, while LOP-loaded 8D3-functionalized nanoparticles NP (0.1, 8D3) resulted in a time increase of around 12 s, showing significant differences between the pre- and post-latency times. These results clearly indicated that both NP (0.1) and NP (0.1, 8D3) produced central analgesia. From these results, it can be confirmed that both types of nanoparticles crossed the BBB although in a different extent, higher for NP (0.1, 8D3), as expected, since they have the active BBB vectorization.

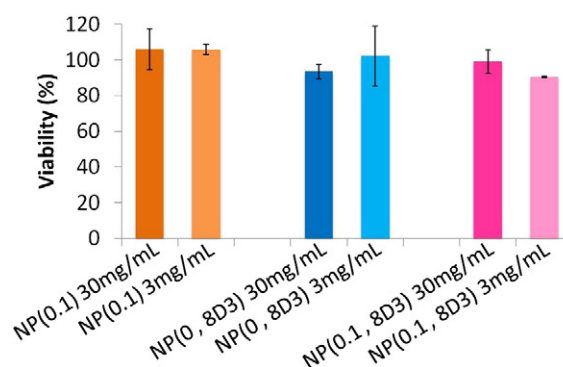


**Fig. 5.** Viability (in %) of HeLa cells, after 24 h of incubation with different sets of nanoparticles, at the as-prepared and use concentrations.

In addition, the analgesic effects were also quantified via the percentage of the maximal possible anti-nociceptive effect produced (% MPE). For this reason, in the present work, analgesia has been also quantified using this value. As Fig. 7 shows, most negative controls (PBS, aqueous morphine, NP (0) and NP (0, 8D3)) produced percentages of analgesia lower than 15%. However, the other negative control, the aqueous polysorbate 80 solution, showed MPE values of around 33%, which was attributed to the permeabilization of the BBB caused by this surfactant [42,50,67]. Both positive controls (aqueous morphine and aqueous polysorbate 80 + LOP) resulted in the higher MPE values, as expected. It is worth remarking that the MPE value of the micellar loperamide solution (aqueous polysorbate 80 with loperamide) achieved the highest MPE values, around 80%, which was previously described in other studies and attributed to the combined effect of the drug with the permeabilization of the BBB produced by the surfactant [42,50,67]. The tested nanoparticles without the antibody, NP (0.1), produced a 25% MPE, which is significantly different than those of most negative controls.

#### 4. Discussion

This study aimed at the design of polymeric nanoparticles, by nano-emulsion templating using low-energy methods, apt for intravenous (*i.v.*) administration with the purpose to target the blood–brain barrier (BBB) and achieve the pharmacological activity at a central nervous system (CNS) level. The nanoparticles have to accomplish several safety requirements for the *i.v.* administration. One of the most important requirements is a nanometric size, below 1  $\mu$ m, to avoid embolization

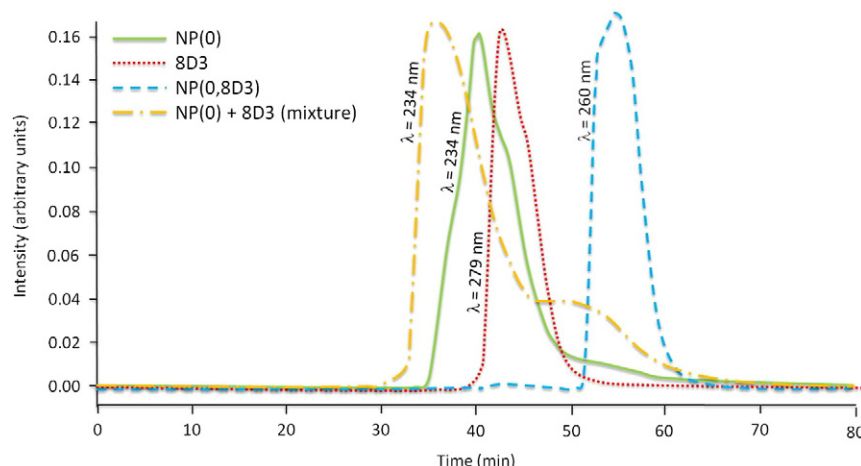


**Fig. 4.** SEC chromatograms of: a) NP (0), b) 8D3; c) NP (0,8D3) (12.5/1); and d) physical mixture of NP (0) + 8D3 (12.5 + 1 in molar ratio).

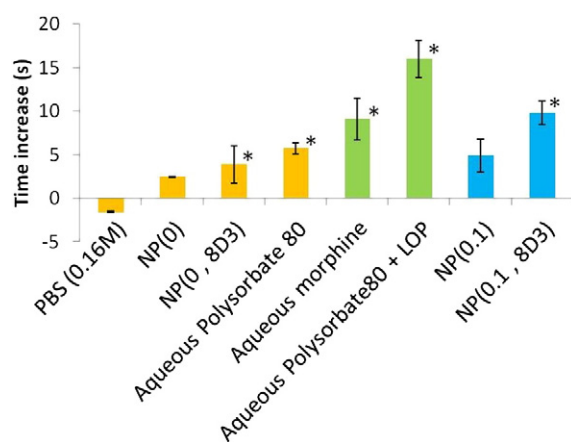


**Fig. 6.** Time differences (in s) from the post-latency time and the pre-latency time of mice of negative controls (yellow), positive controls (green) and test nanoparticles (blue). Stars indicate samples where significant differences were found from the pre- and post-latency time, assessed by the paired-sample t-test.

problems [55,56]. This has been accomplished using a novel approach, not yet used in the context of neurodegeneration treatment research: a low-energy emulsification method, the PIC method, to formulate the template nano-emulsions which allow controlling nano-emulsion size and consequently the size of the resulting nanoparticles after solvent evaporation. It has been shown in previous studies that the physico-chemical properties of nanoparticles are dependent on their template nano-emulsions [28,29,46,47]. A model nano-emulsion system composed of PBS 0.16 M (W)/polysorbate 80 (S)/[4 wt.% PLGA in ethyl acetate] (O) used in a previous study [46] was chosen. However, the use of loperamide in the current study and its low solubility in ethyl acetate required the incorporation of a secondary solvent (ethanol). Compared to the nano-emulsion model system (without ethanol) [46], nano-emulsion formation domain is enhanced by the presence of ethanol as a secondary solvent, which could be explained by a change in the partition coefficient of the surfactant between the oil and the water phases, producing a synergistic effect between the components and favoring the nano-emulsion formation to lower water contents and broader O/S ratios [57,58]. The results shown in Fig. 1 evidenced that the incorporation of 0.1 wt.% of loperamide to the system produced a

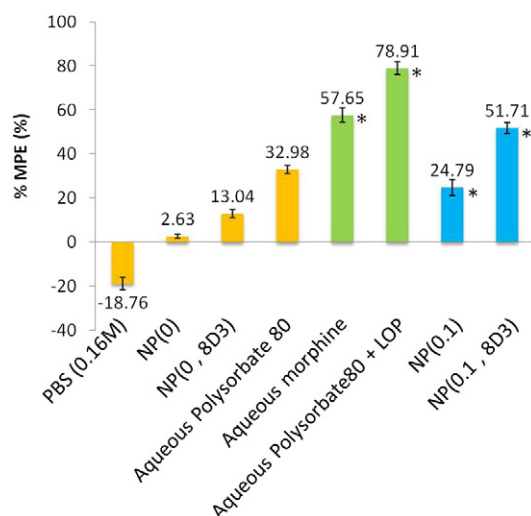


**Fig. 7.** Maximal possible anti-nociceptive effect (MPE, in %), performed with the pre- and post-treatment latency times for each group. Labels indicate the mean % MPE. Stars indicate MPE values that showed significant differences with three of the negative controls (PBS, NP (0), NP (0,8D3)). P-values of this statistic test are in Table S5, from SI.

shrinkage of the nano-emulsion domain. This effect was previously described for other drugs [39,59,60]. The nano-emulsions selected as nanoparticle templates, with 90 wt.% of aqueous phase and 70/30 O/S ratio (and consequently with a low surfactant content (3 wt.%)), showed small nanometric sizes (hydrodynamic radii around 45 nm). The incorporation of loperamide in the oil phase of these nano-emulsions increased droplet hydrodynamic radii from around 45 nm up to values of around 120 nm. Higher percentages of loperamide could be encapsulated, but they produced a higher size increase, not desired for the BBB crossing. The droplet size increase as a result of drug incorporation, proportional to the drug concentration, is a phenomenon described for other drugs [39,59,60], and attributed to the disturbance of the drug on the nano-emulsification process. Specifically, in the present work, it could be due to the combination of two effects: the presence of the secondary solvent together with the addition of the drug. Nevertheless, it is worth noting that nano-emulsion sizes remain in the i.v. administrable range [55,56].

Although the encapsulation efficiency of the drug was very high (>99 wt.%), attributed to the nanoparticle preparation by the nano-emulsion templating approach as well as to loperamide low solubility in the aqueous phases (Table S6, SI), therapeutic doses of loperamide were not achieved in the as-prepared nanoparticles. Higher concentrations of loperamide could not be incorporated in the oil phase due to the limited solubility of the drug in this phase. Nevertheless, with a simple concentration step, followed by dialysis, nanoparticles were concentrated achieving therapeutic concentrations without modifying their physico-chemical properties (Figure S2, SI).

The loperamide release, studied in vitro from the nanoparticle dispersion, and compared to that from a micellar and an aqueous solution, showed unexpected results. Usually, the drug is entirely released from polymeric nanoparticles after long times [39,59–61]. This was observed for the aqueous solution, where loperamide was completely released within 5 days (Fig. 3). However, in here, the micellar solution, that usually releases all entrapped drug, retained around 25% of loperamide in the same period of time. In addition, NP (0.1) nanoparticles retained around 85% loperamide, resulting in a release of only 15% of the drug after 5 days. The retention of the drug in micelles could be attributed to interaction of the drug with surfactant molecules. In addition, for the nanoparticles, the polymeric matrix, where loperamide is entrapped, represents a bigger constraint for its release. The PLGA polymer is hydrophobic, as loperamide, thus preventing loperamide release due to the affinity of the drug for a hydrophobic environment. Accordingly, PLGA was not degraded during this period of time, thus contributing to the constrained release caused by the polymeric matrix (Figure S7, SI). Although interaction of loperamide with polysorbate 80 could be also hypothesized, it was ruled out, as concluded from the similar retention times of the drug in the chromatogram, due to the chromatogram obtained for the release from both, nanoparticle dispersion and micellar solution. The reduced drug release was previously described using other types of colloidal systems and was attributed to the physical obstruction produced by them [61]. The low and very slow loperamide release was first interpreted as a drawback for in vivo use, as unavailability of this drug by the body could be predicted. However, the results of analgesia produced by loperamide (discussed below) enabled to rule out this hypothesis. The pharmacological activity of loperamide could be attributed to an enhanced release due to PLGA biodegradation, thus enabling pharmacological effects in vivo. The low and sustained loperamide release could be regarded as an advantage, since it would enable a longer duration of pharmacological effects. Since PLGA is a biodegradable polymer, it is expected to be degraded in contact with biological tissues, and hence drug release may be enhanced in in vivo conditions.

Concerning toxicity issues, the formulated nanoparticles did not produce cytotoxicity and previous results [53] had showed that they neither produced hemolysis at the required therapeutic concentration (NP concentration = 2 mM), and, as demonstrated by our previous



study [53] they interacted weakly with blood components, independently of the loading/functionalization. Therefore, a long-blood half-life is hypothesized for these nanoparticles, enabling them to arrive to the BBB without damaging tissues nor blood components.

The final goal of the present work, PLGA nanoparticle BBB crossing, is a key issue under current investigation, since neurological diseases treatment usually lacks efficacy due to the limited amount of drug that reaches the central nervous system (CNS). As described in the [Results](#) section, the 8D3 monoclonal antibody was attached to the nanoparticle surface in order to enhance the BBB crossing, since this is an antibody against the transferrin receptor, overexpressed in the BBB [62–64]. It is worth noting that sizes of the 8D3-functionalized nanoparticles ([Table 3](#)) are maintained within the range of those appropriate to cross the BBB by passive diffusion, which is also an indication of nanoparticle integrity in spite of the pH changes in the covalent attachment step (see [Section 2.2.6](#)). In addition, their reduced size enables longer blood half-time [62,64]. Concerning their surface charge, although BBB endothelial cells are negatively charged, previous studies confirmed that receptor mediated transcytosis is a process independent of nanoparticle charge [62,64].

The nanoparticle surface functionalization with the 8D3 antibody was confirmed by SEC (see [Fig. 4](#)), a technique that enables the separation of compounds as a function of their hydrodynamic size (not only their molecular weight) [65].

Concerning *in vivo* studies, it was demonstrated by measuring the MPE percentage that both sets of nanoparticles, NP (0.1) and NP (0.1, 8D3), were able to cross the BBB, although in a different extent. Previous studies on the design of polymeric nanoparticles intended to cross the BBB evaluated the BBB crossing by measuring analgesia [29,30,32,42]. Loperamide, in current pharmaceutical dosages, is used as an antidiarrheal drug, since, without any specific vectorization, it ends up in the gastrointestinal tract, due to its inability to cross the BBB and its lack of central effects production. However, with a specific targeting to the BBB that enables loperamide arrival to the central nervous system, it can produce central analgesia, as evidenced in previous studies [10, 30–32]. Since the hot plate test measures the supraspinal analgesia, which has a central origin, the selection of loperamide was found appropriate to study the BBB crossing. Analgesia quantified by means of measuring %MPE, as described in the [Results](#) section, enabled to confirm an analgesic effect for the designed nanoparticles. In addition, after their functionalization with the covalent antibody attachment, demonstrated by SEC ([Fig. 4](#)), the MPE value increased notably, as previously described [31]; it was around 52%, which is nearly the same than the positive morphine control (57%). The specific vectorization of the nanoparticles to the BBB must be caused by the 8D3 antibody, since it is the only compound that was not present in non-functionalized nanoparticles. In addition, this specific vectorization is also a proof of the maintenance of antibody structure and functionality after the covalent reaction. Therefore, the antibody nanoparticle functionalization enabled an efficient BBB crossing, comparable to positive controls. These results are a clear proof of the capability of the designed PLGA nanoparticles to transport drugs to the CNS.

Although functionalized nanoparticles did not produced as high analgesic values as those obtained for the aqueous polysorbate 80 + LOP, they did produce a higher analgesia than negative controls, thus confirming their capability to transport drugs across the BBB. The use of nanoparticles over aqueous polysorbate 80 is advantageous in terms of controlled drug release (sustained, enabling longer pharmacological activity) and specific BBB penetration through transferring receptors by receptor mediated transcytosis. In addition, although polysorbate 80 is FDA approved for the parenteral administration, the concentrations required in the micellar solution to solubilize LOP were higher than those used in the nanoparticle dispersion, which is not desirable.

Comparing the results of the analgesic test with previous bibliography [30–32] for example, Alyautdin et al., [31] studied poly(butyl

cianoacrylate) (PBCA) nanoparticles, without or with a polysorbate 80 coating, after nanoparticle preparation; with a loperamide concentration similar to that of the present work (2.7 mg/kg). They obtained MPE values of around 27% after the polysorbate coating, which are very similar to our results. In addition, when they tried the micellar solution of polysorbate 80 with loperamide, they also found higher MPE values than those reported for positive controls. However, the effect produced for the micellar solution disappeared rapidly, while the effect from the nanoparticle dispersion was maintained. Although we did not study analgesia at longer times, which would be interesting in further studies, a prolonged drug effect could be also hypothesized for our nanoparticles due to the slow release found for the nanoparticle dispersion ([Fig. 3](#)). Other studies administered *i.v.* PLGA nanoparticles to produce central analgesia, since this polymer is appropriate for the central nervous system treatment [30,32]. Those nanoparticles without polysorbate 80 [32] produced lower levels of analgesia than those reported in the present work. However, when PLGA nanoparticles were coated with polysorbate 80 [30], analgesia increased up to around 80% MPE values. Although the analgesia found by these authors is higher than those found in the present study, it should be mentioned that they used a markedly higher dose of loperamide (7 mg/kg in front of our 3 mg/kg).

Compared to those studies, nanoparticles reported here are advantageous from different points of view. Concerning physico-chemical properties, nanoparticles formulated in the present study have smaller sizes than those reported in previous bibliography [30,31]. In terms of nanoparticle preparation, our strategy represents a novel advantage not only for the use of low-energy emulsification methods, energy- and cost-efficient, easily scalable, but also for the incorporation of the polysorbate 80 surfactant as a part of the formulation, avoiding a coating step. Moreover, all components used are FDA approved. It is worth noting that nanoparticles designed in the present work were intended to cross the BBB, which was successfully achieved.

## 5. Conclusions

The present work demonstrated that loperamide, loaded in PLGA nanoparticles (prepared by nano-emulsion templating, using a low-energy method) is efficiently transported to the CNS through the BBB when it is encapsulated in nanoparticles containing traces of polysorbate 80, specifically if nanoparticles are functionalized with the antibody against the transferring receptor, overexpressed in the BBB.

To achieve this purpose, a wide study of template non-loaded polymeric O/W nano-emulsions was performed. Nano-emulsions with 90 wt.% of aqueous phase content and 70/30 O/S ratio was selected as a compromise between small droplet sizes (50 nm) and low surfactant contents. This nano-emulsions were reformulated to include 0.1 wt.% LOP in the oil phase, resulting in droplet sizes around 100 nm, appropriate for the intravenous administration. Compared with previous studies, in our work, the polysorbate 80 surfactant, which permeabilizes the BBB, was a part of the nanoparticle formulation, which avoids further coating steps that usually are cost and time ineffective. In addition, the nanoparticles able to cross the BBB were produced by a low-energy nano-emulsification approach (the PIC method), an easily scalable methodology, appropriate for the pharmaceutical industries. Therefore, a novel scalable procedure to produce nanoparticles able to cross the BBB has been described.

## Acknowledgments

Financial support from MINECO (grants CTQ2011-29336-CO3-O1); Generalitat de Catalunya (grant 2009-SGR-961), and CIBER-BBN are acknowledged. CIBER-BBN is an initiative funded by the VI National R&D&I Plan 2008–2011, Iniciativa Ingenio 2010, Consolider Program, CIBER Actions and financed by the Instituto de Salud Carlos III with assistance from the European Regional Development Fund. Cristina



Fornaguera is grateful to AGAUR for their Predoctoral Fellowship (grant FI-DGR 2012). Authors acknowledge Adele Alagia and Dr. Santiago Grijalvo for their kind support in the preparation of cell culture experiments. Authors also acknowledge Alba Ortega for her kind support in part of the experiments.

## Appendix A. Supplementary data

Supplementary data to this article can be found online at <http://dx.doi.org/10.1016/j.jconrel.2015.06.002>.

## References

- [1] J.K. Sahni, S. Doggui, J. Ali, S. Baboota, L. Dao, C. Ramassamy, Neurotherapeutic applications of nanoparticles in Alzheimer's disease, *J. Control. Release* 152 (2011) 208–231.
- [2] M.R. Farlow, Pharmacokinetic profiles of current therapies for Alzheimer's disease: implications for switching to galantamine, *Clin. Ther.* 23 (A) (2001) 13–24.
- [3] G. Tosi, R.A. Fano, L. Bondioli, L. Badiali, R. Benassi, F. Rivasi, B. Ruozzi, F. Forni, A. Vandelli, Investigation on mechanisms of glycopeptide nanoparticles for drug delivery across the blood–brain barrier, *Nanomedicine* 6 (3) (2011) 423–436.
- [4] M. Gregori, M. Masserini, S. Mancini, *Nanomedicine for the treatment of Alzheimer's disease*, *Nanomedicine (Lond)* 10 (7) (2015) 1203–1218.
- [5] S. Lilienfeld, Galantamine – a novel cholinergic drug with a unique dual mode of action for the treatment of patients with Alzheimer's disease, *CNS Drug Rev.* 8 (2) (2006) 159–176.
- [6] M. Villaroya, A.G. García, J. Marco-Contelles, M.G. López, An update on the pharmacology of galantamine, *Expert Opin. Invest. Drugs* 16 (12) (2007) 1987–1998.
- [7] M. Fazil, S. Baboota, J.K. Sahni, J. Ali, Nanotherapeutics for Alzheimer's disease (AD): past, present and future, *J. Drug Target.* 20 (2) (2012) 97–113.
- [8] J. Todoroff, R. Vanbever, Fate of nanomedicines in the lungs, *Curr. Opin. Colloid Interface Sci.* 16 (2011) 246–254.
- [9] C. Pinto Reis, R.J. Neufeld, A.J. Ribeiro, F. Veiga, Nanoencapsulation I. Methods for preparation of drug-loaded polymeric nanoparticles, *Nanomed.: Nanotechnol. Biol. Med.* 2 (1) (2006) 8–21.
- [10] B. Neha, B. Ganesh, K. Preeti, Drug delivery to the brain using polymeric nanoparticles: a review, *Int. J. Pharm. Life Sci.* 2 (3) (2013) 107–132.
- [11] Y. Aktas, M. Yemisci, K. Andrieux, R.N. Gursoy, M.J. Alonso, E. Fernandez-Megia, et al., Development and brain delivery of chitosan-PEG nanoparticles functionalized with the monoclonal antibody OX26, *Bioconjugate Chem.* 16 (2005) 1503–1511.
- [12] C. Vauthier, K. Bouchemal, Methods for the preparation and manufacture of polymeric nanoparticles, *Pharm. Res.* 26 (5) (2009) 1025–1058.
- [13] V.P. Torchillin, Multifunctional nanocarriers, *Adv. Drug Deliv. Rev.* 64 (2012) 302–315.
- [14] M. Willert, R. Rothe, K. Landfester, M. Antonietti, Synthesis of inorganic and metallic nanoparticles by miniemulsification of molten salts and metals, *Chem. Mater.* 13 (2001) 4681–4685.
- [15] N. Anton, J.P. Benoit, P. Saulnier, Design and production of nanoparticles formulated from nano-emulsion templates: a review, *J. Control. Release* 128 (2008) 185–199.
- [16] C. Solans, P. Izquierdo, J. Nolla, N. Azemar, M.J. García-Celma, Nano-emulsions, *Curr. Opin. Colloid Interface Sci.* 10 (2005) 102–110.
- [17] T. Tadros, P. Izquierdo, J. Esquena, C. Solans, Formation and stability of nano-emulsions, *Adv. Colloid Interface Sci.* 108–109 (2004) 303–318.
- [18] N. Anton, T.F. Vandamme, The universality of low-energy emulsification, *Int. J. Pharm.* 377 (2009) 142–147.
- [19] A. Forgiarini, J. Esquena, C. González, C. Solans, Formation of nano-emulsions by low-energy emulsification methods at constant temperature, *Langmuir* 17 (2001) 2076–2083.
- [20] I. Solè, A. Maestro, C.M. Pey, C. González, C. Solans, J.M. Gutiérrez, Nano-emulsions preparation by low energy methods in an ionic surfactant system, *Colloids Surf. A Physicochem. Eng. Asp.* 288 (2006) 138–143.
- [21] L. Wang, K.J. Mutch, J. Eastoe, R.K. Heenan, J. Dong, Nanoemulsions prepared by a two-step low-energy process, *Langmuir* 24 (2008) 6092–6099.
- [22] L. Wang, R. Tabor, J. Eastoe, X. Li, R.K. Heenan, J. Dong, Formation and stability of nanoemulsions with mixed ionic–nonionic surfactants, *Phys. Chem. Chem. Phys.* 11 (2009) 9772–9778.
- [23] H.J. Yang, W.G. Cho, S.N. Park, *J. Ind. Eng. Chem.* 15 (2009) 331–335.
- [24] S. Desgouilles, C. Vauthier, D. Bazile, J. Vacus, J.L. Grossiord, M. Veillard, P. Couvreur, *Langmuir* 19 (2003) 9504.
- [25] X. Song, Y. Zhao, S. Hou, F. Xu, R. Zhao, J. He, Z. Cai, Y. Li, Q. Chen, *Eur. J. Pharm. Biopharm.* 69 (2008) 445.
- [26] M.C. Venier-Julienne, J.P. Benoit, *Pharm. Acta Helv.* 71 (1996) 121.
- [27] D. Moinard-Chérot, Y. Chevalier, S. Briançon, L. Beney, H. Fessi, *J. Colloid Interface Sci.* 317 (2008) 458.
- [28] G. Calderó, M.J. García-Celma, C. Solans, Formation of polymeric nano-emulsions by a low energy method and their use for nanoparticle preparation, *J. Colloid Interface Sci.* 353 (2011) 406–411.
- [29] R.N. Alyautdin, V.E. Petrov, K. Langer, A. Berthold, D.A. Kharkevich, J. Kreuter, Delivery of loperamide across the blood–brain barrier with polysorbate 80-coated polybutylcyanoacrylate nanoparticles, *Pharm. Res.* 14 (3) (1997) 325–328.
- [30] S. Gelperina, O. Maksimenko, A. Khalansky, L. Vanchugova, E. Shipulo, K. Abbasova, R. Berdiev, S. Wohlfart, N. Chepurnova, J. Kreuter, Drug delivery to the brain using surfactant-coated poly(lactide-co-glycolide) nanoparticles: influence of the formulation parameters, *Eur. J. Pharm. Biopharm.* 74 (2010) 157–163.
- [31] K. Ulbrich, T. Hekmatara, E. Herbert, J. Kreuter, Transferrin- and transferring-receptor-antibody-modified nanoparticles enable drug delivery across the blood–brain barrier (BBB), *Eur. J. Pharm. Biopharm.* 71 (2009) 251–256.
- [32] G. Tosi, L. Costantino, F. Rivasi, B. Ruozzi, E. Leo, A.V. Vergoni, R. Tacchi, A. Bertolini, M.A. Vandelli, F. Forni, Targeting the central nervous system: in vivo experiments with peptide-derivatized nanoparticles loaded with Loperamide and Rhodamine-123, *J. Control. Release* 122 (2007) 1–9.
- [33] USP Pharmacopoeia, On-line resource accessible at: <http://www.usp.org/2014>.
- [34] W. Schärft, in: H. Pasch (Ed.), *Light Scattering From Polymer Solutions and Nanoparticle Dispersions*, Springer laboratory, ISBN: 978-3-540-71951-9 2006, p. 22.
- [35] A.V. Delgado, F. González-Caballero, R.J. Hunter, L.K. Koopal, Measurement and interpretation of electrokinetic phenomena, *J. Colloids Interface Sci.* 309 (2007) 194–224.
- [36] I.I. Hewala, Spectrofluorimetric and derivative absorption spectrophotometric techniques for the determination of loperamide hydrochloride in pharmaceutical formulations, *J. Pharm. Biomed. Anal.* 13 (6) (1995) 761–767.
- [37] C. Gómez-Gaete, N. Tsapis, M. Besnard, A. Bochot, E. Fattal, *Int. J. Pharm.* 331 (2007) 153.
- [38] N. Schafroth, C. Arpagaus, U. Yadhav, S. Makne, D. Doroumis, *Colloid Surf. B* 90 (2012) 8, <http://dx.doi.org/10.1016/j.colsurfb.2011.09.038>.
- [39] C. Fornaguera, M. Llinàs, C. Solans, G. Calderó, Design and in vitro evaluation of bio-compatible dexamethasone-loaded nanoparticle dispersions, obtained from nano-emulsions, for inhalatory therapy, *Colloid Surf. B* 125 (1) (2015) 58–64, <http://dx.doi.org/10.1016/j.colsurfb.2014.11.006>.
- [40] H. Edelhoch, Spectroscopic determination of tryptophan and tyrosine in proteins, *Biochemistry* 6 (7) (1967) 1948–1954.
- [41] D. Putnam, C.A. Gentry, D.W. Pack, R. Langer, Polymer-based gene delivery with low cytotoxicity by unique balance of side-chain termini, *PNAS* 98 (3) (2001) 1200–1205.
- [42] Y.-C. Chen, W.-Y. Hsieh, W.-F. Lee, D.-T. Zeng, Effects of surface modification of PLGA-PEG-PLGA nanoparticles on loperamide delivery efficiency across the blood–brain barrier, *J. Biomater. Appl.* 27 (7) (2011) 909–922.
- [43] B.P. Kirby, R. Pabari, C.N. Chen, Baharna M. Al, J. Walsh, Z. Ramtoola, Comparative evaluation of the degree of pegylation of poly(lactic-co-glycolic acid) nanoparticles in enhancing central nervous system delivery of loperamide, *J. Pharm. Pharmacol.* 65 (2013) 1473–1481.
- [44] Z. Chen, E. Davies, W.S. Miller, S. Shan, K.J. Valenzano, D.J. Kyle, Design and synthesis of 4-phenyl piperidine compounds targeting the mu receptor, *Bioorg. Med. Chem. Lett.* 14 (21) (2004) 5275–5279.
- [45] A. Goldstein, A. Naidu, Multiple opioid receptors: ligand selectivity profiles and binding site signatures, *Mol. Pharmacol.* 36 (2) (1989) 265–272.
- [46] C. Fornaguera, S. Grijalvo, M. Galán, E. Fuentes-Paniagua, F.J. de la Mata, R. Gómez, R. Eritja, G. Calderó, C. Solans, Novel non-viral gene delivery systems composed of carbosilane dendron functionalized nanoparticles prepared from nano-emulsions as non-viral carriers for antisense oligonucleotides, *Int. J. Pharm.* 478 (2015) 113–123.
- [47] C. Solans, I. Solè, Nano-emulsions: formation by low-energy methods, *Curr. Opin. Colloid Interface Sci.* 17 (2012) 246–254.
- [48] M. Jayne Lawrence, Surfactant systems: their use in drug delivery, *Chem. Soc. Rev.* 23 (1994) 417–424.
- [49] J. Kreuter, Nanoparticulate systems for brain delivery of drugs, *Adv. Drug Deliv. Rev.* 64 (2012) 213–222.
- [50] S. Wohlfart, S. Gelperina, J. Kreuter, Transport of drugs across the blood–brain barrier by nanoparticles, *J. Control. Release* 161 (2) (2012) 264–273.
- [51] A.V. Kabanov, H.E. Gendelman, Nanomedicine in the diagnosis and therapy of neurodegenerative disorders, *Prog. Polym. Sci.* 32 (2007) 1054–1082.
- [52] S.K. Sahoo, V. Labhasetwar, Enhanced antiproliferative activity of transferrin conjugated, paclitaxel-loaded nanoparticles is mediated via sustained intracellular drug retention, *Mol. Pharm.* 2 (2005) 373–383.
- [53] C. Fornaguera, G. Calderó, M. Mitjans, P. Vinardell, C. Solans, C. Vauthier, interaction of PLGA nanoparticles with blood components: protein adsorption, coagulation, activation of the complement system and hemolysis studies, *Nanoscale* (2015), <http://dx.doi.org/10.1039/c5nr00733j>.
- [54] J.L. Jiménez, M.I. Clemente, N.D. Weber, J. Sánchez, P. Ortega, F.J. de la Mata, R. Gómez, D. García, L.A. López-Fernández, M.A. Muñoz-Fernández, Carbosilane dendrimers to transfect human astrocytes with small interfering RNA targeting human immunodeficiency virus, *Biodrugs* 24 (5) (2010) 331–343.
- [55] M.A. Dobrovolskaia, S. McNeil, Handbook of immunological properties of engineered nanomaterials, *Frontiers in Nanobiomedical Research*, SAIC-Frederick, Inc., USA, 2013.
- [56] R. Gref, A. Domb, P. Quellec, T. Blunk, R.H. Müller, J.M. Verbavatz, R. Langer, The controlled intravenous delivery of drugs using PEG-coated sterically stabilized nanoparticles, *Adv. Drug Deliv. Rev.* 64 (2012) 316–326.
- [57] N. Anton, J.-P. Benoit, P. Saulnier, Design and production of nanoparticles formulated from nano-emulsions – a review, *J. Control. Release* 128 (3) (2008) 185–199.
- [58] D. Morales, J.M. Gutiérrez, M.J. García-Celma, C. Solans, A study of the relation between bicontinuous microemulsions and oil/water nano-emulsion formation, *Langmuir* 19 (2003) 7196–7200.
- [59] A.A. Date, M.S. Nagarsenker, Design and evaluation of self-nanoemulsifying drug delivery systems (SNEDDS) for cefpodoxime pexetil, *Int. J. Pharm.* 329 (2007) 166–172.
- [60] A.A. Date, N. Desai, R. Dixit, M. Nagarsenker, Self-nanoemulsifying drug delivery systems: formulation insights, applications and advances, *Nanomedicine* 5 (10) (2010) 1595–1616.

- [61] G. Calderó, M. Llinàs, M.J. García-Celma, C. Solans, Studies on controlled release of hydrophilic drugs from W/O high internal phase ratio emulsions, *J. Pharm. Sci.* 99 (2) (2010) 701–711.
- [62] R. Gabathuler, Approaches to transport therapeutic drugs across the blood–brain barrier to treat brain diseases, *Neurobiol. Dis.* 37 (2010) 48–57.
- [63] J. Nicolas, S. Mura, D. Brambilla, N. Mackiewicz, P. Couvreur, Design, functionalization strategies and biomedical applications of targeted biodegradable/biocompatible polymer-based nanocarriers for drug delivery, *Chem. Soc. Rev.* 42 (2013) 1147–1235.
- [64] R. Alyautdin, I. Khalin, M.I. Nafeeza, M.H. Haron, D. Kuznetsov, Nanoscale drug delivery systems and the blood–brain barrier, *Int. J. Nanomedicine* 9 (2014) 795–811.
- [65] K. Rebolj, D. Pahovnik, E. Zagar, Characterization of a protein conjugate using an asymmetrical-flow field-flow fractionation and a size-exclusion chromatography with multi-detection system, *Anal. Chem.* 84 (2012) 7374–7383.
- [66] E. Catiker, M. Gümüşderelioglu, A. Güner, Degradation of PLA, PLGA homo- and copolymers in the presence of serum albumin: a spectroscopic investigation, *Polym. Int.* 49 (2000) 728–734.
- [67] J. Kreuter, Mechanism of polymeric nanoparticle-based drug transport across the blood–brain barrier (BBB), *J. Microencapsul.* 30 (1) (2013) 49–54.